Smallest Metallic Nanorods Using Physical Vapor Deposition

Xiaobin Niu,[1] Stephen P. Stagon,[1] Hanchen Huang,[1,*] J. Kevin Baldwin,[2] and Amit Misra[2]
[1]*Department of Mechanical Engineering, University of Connecticut, Storrs, Connecticut 06269, USA*
[2]*Los Alamos National Laboratory, MS K771, Los Alamos, New Mexico 87545, USA*

(Received 23 January 2013; published 28 March 2013)

Physical vapor deposition provides a controllable means of growing two-dimensional metallic thin films and one-dimensional metallic nanorods. While theories exist for the growth of metallic thin films, their counterpart for the growth of metallic nanorods is absent. Because of this absence, the lower limit of the nanorod diameter is theoretically unknown; consequently the experimental pursuit of the smallest nanorods has no clear target. This Letter reports a closed-form theory that defines the diameter of the smallest metallic nanorods using physical vapor deposition. Further, the authors verify the theory using lattice kinetic Monte Carlo simulations and validate the theory using published experimental data. Finally, the authors carry out a series of theory-guided experiments to grow well-separated metallic nanorods of ∼10 nm in diameter, which are the smallest ever reported using physical vapor deposition.

DOI: 10.1103/PhysRevLett.110.136102 PACS numbers: 68.65.La, 02.70.Uu, 61.46.Km, 68.55.A−

The growth of metallic nanorods, which are generally also crystalline, using physical vapor deposition (PVD) allows the control of crystalline structures and chemical composition [1,2]. Like in the growth of other materials, it is desirable to grow ever smaller nanorods to maximize their nanoscale functionalities [3–6]. The question is what is the smallest nanorod possible using PVD? One may expect that the growth theories of crystalline thin films [7–9] apply to the growth of metallic nanorods, since the two processes bear similarities. In contrast to the growth of crystalline thin films, the growth of metallic nanorods is dictated by the dynamics of multiple-layer surface steps; this differentiation is not addressed by the existing theories of thin film growth. Consequently, the growth theories of crystalline thin films are not applicable to the growth of metallic nanorods [10]. Without a theoretical foundation of nanorod growth, the physical limit of the smallest diameter is unknown. As a result, the pursuit of the smallest nanorods has no clear target, and consequently no clear path to the target.

In this Letter, we present (1) a closed-form theory of the smallest diameter, (2) verification of the theory using lattice kinetic Monte Carlo (LKMC) simulations and validation using previous experiments, and (3) the realization of the smallest nanorods using theory-guided PVD experiments.

For the theoretical formulation, the conceptual framework of nanorod growth serves as the starting point [10]. In contrast to the theories for the growth of large crystals [7–9], this framework recognizes that multiple-layer surface steps are kinetically stable [11]; in contrast, the classical theory predicts that such steps are kinetically unstable [12]. Further, these multiple-layer surface steps dictate the diffusion of adatoms during nanorod growth [13–15]. Under this framework, metallic nanorods grow in two modes—I and II (Fig. 1). In mode I, the growth takes place on wetting substrates and nanorods have the shape of a tower [16]. The competition between multiple-layer and monolayer surface steps defines the diameter of nanorods, and also defines the slope on the side of nanorods. The diameter becomes smaller if more of the surface steps are multiple-layer instead of monolayer. In mode II, the growth takes place on nonwetting substrates and nanorods have the shape of a cylinder (or of an inverted tower if they grow sufficiently tall). Because of the complete, or nearly complete, dominance of multiple-layer surface steps over monolayer surface steps, growth mode II results in the smallest diameter of nanorods.

Focusing on growth mode II, we first describe our physical model of nanorod growth; the mathematical formulation then turns the model into a closed-form theory. The model starts with nucleation on a nonwetting substrate [snapshot t_1 in Fig. 1(b)]. Because of nonwettability, the critical size of nucleating the second layer is one atomic diameter. Aiming at the smallest diameter, we consider the complete geometrical shadowing condition—that is, atoms are deposited onto only the top of nanorods, not onto the sides. Once the deposited atoms overcome the large diffusion barrier of multiple-layer steps, they experience much smaller diffusion barriers on the sides and therefore tend to distribute equally along the vertical direction. As a result, they have the shape of a cylinder [snapshot t_2 in Fig. 1(b)]. Since the diameter of the nanorods is small, only one adatom will be on top most of the time, and a new layer nucleates once two adatoms present simultaneously; this is also called the lone adatom model [9]. The snapshot t_2 in Fig. 1(b) shows the configuration with the nucleus of a new layer. With the small diameter of nanorods and the large diffusion barrier at the multiple-layer steps or edges of the nanorods, the newly nucleated layer will grow to full coverage before any deposited atoms diffuse to the side. The snapshot t_3 in Fig. 1(b) shows the configuration when the coverage of one layer is complete. The snapshot t_4 in

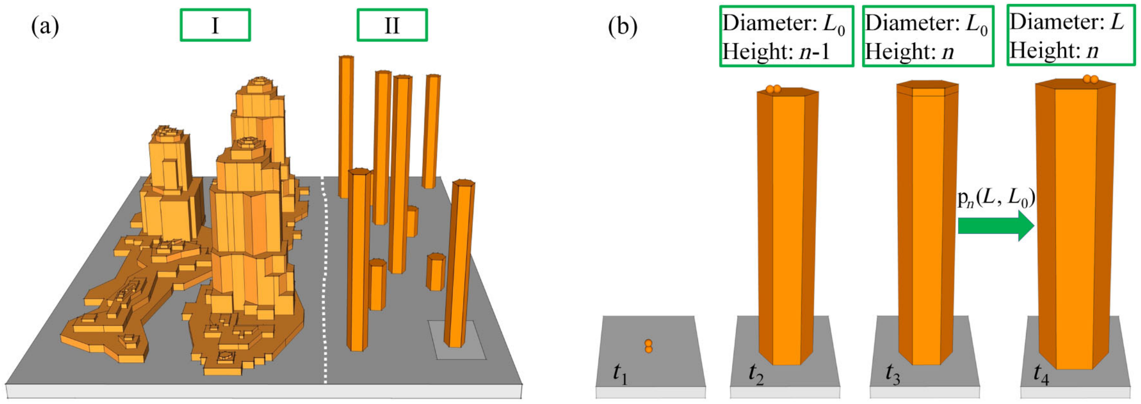

FIG. 1 (color online). (a) Schematic of the two modes of nanorod growth, with mode II giving rise to the smallest nanorods; and (b) evolution of a nanorod, corresponding to the boxed one in (a), as a function of time for mode II.

Fig. 1(b) is similar to the snapshot t_2, except with one extra layer on top of the nanorod.

Based on the physical model of nanorod growth, the clock in our theoretical formulation starts at the moment when the coverage of the nth layer has just been completed [snapshot t_3 in Fig. 1(b)]. The cross-sectional area is $A = \alpha L^2$ with L being L_0 at this moment. The α is a geometrical factor: $\alpha = \pi/4$ for circular cross sections and $\alpha = 1$ for square cross sections. For easy comparison with experiments, we will refer to L as the "diameter," even though it is precisely diameter only for circular cross sections. Before the next layer is nucleated, the adatoms on top diffuse to the sides of nanorods, leading to lateral growth. During this period of lateral growth, mass conservation requires $\int_0^t F_e \alpha L^2 dt = n\alpha L^2 - n\alpha L_0^2$; F_e is the effective deposition rate on top of the nanorod and t is the time. It should be noted that this conservation equation is valid for mode II of nanorod growth in Fig. 1(a), and that it is different from that for the growth of large crystals [7–9].

Using the conservation equation and following the lone adatom model, we derive the distribution $f_n(L, L_0) = 1 - \exp[(L_0^5 - L^5)/L_n^5]$ as the fraction of nanorods on top of which nucleation has taken place when the diameter of the nanorods is L; details of the derivation are available in Ref. [17]. Here, $L_n = [(10\nu_{3D})/(n\alpha^2 F_e)]^{1/5}$ and ν_{3D} is the diffusion jump rate of adatoms over multiple-layer surface steps. The nucleation probability density that the $(n+1)$th layer starts to nucleate on top of a nanorod of diameter L is then $p_n(L, L_0) = df_n(L, L_0)/dL = \{5L^4 \exp[(L_0^5 - L^5)/L_n^5]\}/L_n^5$.

Next, we consider the fact that not all nanorods have the same diameter L_0 at snapshot t_2 in Fig. 1(b). Instead, if their size distribution is $S_{n-1}(L)$, the size distribution at snapshot t_4 is $S_n(L) = \int_0^L dl S_{n-1}(l) p_n(L, l)$. For a nonwetting substrate, we approximate the size distribution of the first layer as a delta function, $S_1(L) = \delta(L - 0)$. With this approximation, we recursively determine $S_n(L)$. Finally, we determine the peak diameter $L_{\min}$ as the L that satisfies $dS_n(L)/dL = 0$. For a sufficiently narrow size distribution, this peak diameter $L_{\min}$ represents the smallest diameter. When the number of layers n is large, we obtain a closed-form expression $L_{\min} \approx [(10/\alpha^2) \times \ln(n/2)(\nu_{3D}/F_e)]^{1/5}$. Since the effective deposition rate F_e is proportional to the nominal deposition rate F through $F_e = F \sin\theta$ with θ being the incidence angle, $L_{\min} \propto (\nu_{3D}/F)^{1/5}$.

Before using the theory, we verify it here. First, we numerically determine $S_n(L)$ as a function of the number of layers n (effectively time); further details of the verification are available in Ref. [17]. As Fig. 2(a) shows, the peak diameter first increases fast then more slowly with time, and the distribution becomes very narrow as n reaches 2000 layers. The narrow distribution confirms the validity of using the peak diameter as representative of the smallest diameter $L_{\min}$. Further, the numerical solution and the closed-form expression of $L_{\min}$ are nearly identical as nanorods grow to 2000 layers [Fig. 2(a) inset]. LKMC simulations using various substrate temperatures or various deposition rates, while keeping other conditions unchanged, show a nearly identical dependence of $L_{\min}$ on $(\nu_{3D}/F)^{1/5}$ as the theory predicts [Fig. 2(a) inset].

Upon verification of the theoretical formulations, we next use LKMC simulations to test the validity of the theory beyond complete geometrical shadowing conditions. As long as mode II of nanorod growth is operational, we still expect the dominance of multiple-layer surface steps, even if geometrical shadowing is incomplete. Indeed, the simulation results [Fig. 2(b) inset] show the dominance of multiple-layer surface steps. By changing ν_{3D} and F independently, the simulation results show in Fig. 2(b) that $L_{\min}$ is still proportional to $(\nu_{3D}/F)^{1/5}$ when the incidence angle of atomic flux is 85°.

Having verified the theory $L_{\min} \approx [(10/\alpha^2)\ln(n/2) \times (\nu_{3D}/F_e)]^{1/5}$ and extended its applicability as $L_{\min} \propto (\nu_{3D}/F)^{1/5}$ under incomplete geometrical shadowing, we now use a previous experiment [18] to validate it. In the experiment, Cu nanorods of ~30 nm in diameter grow

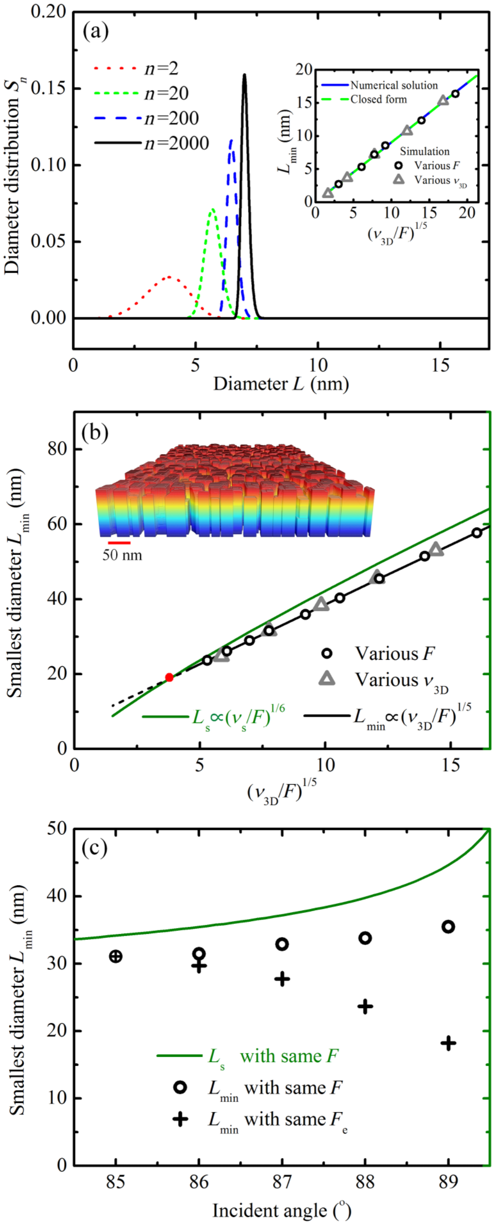

FIG. 2 (color online). (a) The theoretical distribution $S_n(L)$ for various numbers of layers n in height; the inset shows a comparison of the numerical solution, the closed-form expression, and LKMC simulation results under complete geometrical shadowing as a function of $(\nu_{3D}/F)^{1/5}$. (b) LKMC simulation results under incomplete geometry shadowing as a function of $(\nu_{3D}/F)^{1/5}$; the separation of nanorod nuclei L_s is included for comparison, and the incidence angle is 85°. The inset shows nanorods from a LKMC simulation with random nucleation. (c) LKMC simulation results under incomplete geometry shadowing as a function of incidence angle, with either the same $F_e = 1\,\sin 5°$ nm/s or the same $F = 1$ nm/s; the separation of nanorod nuclei L_s is included for comparison.

under a deposition rate of 1 nm/s with an incidence angle of 85°; the substrate temperature is uncontrolled but is within 300–350 K. By increasing the deposition rate to 6 nm/s, the growth of nanorods transitions into the growth of a dense film. By including the theoretical separation of nanorod nuclei L_s [19] in Fig. 2(b), our theory explains this anomalous transition as the following. The crossover of $L_{\min}$ and L_s occurs at ~20 nm. As deposition rate increases, both $L_{\min}$ and L_s decrease. When they reach ~20 nm, L_s becomes smaller than $L_{\min}$, so there is no space for separated nanorods to exist. Because of random nucleation, some nanorods are separated at a smaller distance than the theoretical value L_s. As a result, nanorods bridge and merge even if $L_s > L_{\min}$, provided they both are still close to ~20 nm. That is, L_s makes it nearly impossible to grow well separated Cu nanorods that are smaller than ~30 nm; beyond our own experiments, others have also reported only nanorods of ~30 nm or larger but not smaller [20,21]. The fact that the theory explains the anomalous experimental results serves as a validation.

Now that the theory has been verified and validated, we use it to guide the pursuit of the smallest nanorods. The first insight from the theory is that L_s is the limiting factor of growing smaller nanorods. If we can eliminate the constraint of L_s, it may become possible to grow smaller and well-separated nanorods of diameter $L_{\min}$. It is possible to change L_s with minor impact on $L_{\min}$ by using substrates of different wettability or heterogeneous nucleation, or to change $L_{\min}$ with minor impact on L_s by using different substrate temperatures. Putting this insight into action, we apply four strategies. (1) By using large incidence angles, we lower the effective deposition rate to promote the relationship $L_s > L_{\min}$; (2) by using lower substrate temperatures, we take the advantage of larger activation energy in $L_{\min}$ to promote the relationship $L_s > L_{\min}$; (3) by using substrates with heterogeneous nucleation, we make L_s ineffective; and (4) by using highly nonwetting substrates, we increase L_s to promote $L_s > L_{\min}$. Since the last three strategies are apparent, we use Fig. 2(c) to show the feasibility of only the first strategy. As the incidence angle becomes larger, while keeping the nominal deposition rate constant, $L_{\min}$ becomes larger but L_s becomes even larger. Indeed, the increase of incidence angle promotes $L_s > L_{\min}$.

The second insight is that a decrease of ν_{3D} (by an increase of the diffusion barrier of adatoms over multiple-layer surface steps) can be effective to reduce the diameter of nanorods according to $L_{\min} \propto (\nu_{3D}/F)^{1/5}$. Putting this insight into action, we use quantum mechanics calculations to identify a metal with a large diffusion barrier of adatoms and therefore small ν_{3D}. Our calculations show that the relevant energy barrier of adatoms diffusion down a multiple-layer surface step in Au is 0.52 eV, much larger than the 0.40 eV in Cu or 0.12 eV in Al [14,15]; this barrier is in contrast to the Ehrlich-Schwoebel barrier of adatoms diffusion down a monolayer surface step [12,22]. With this set of data, the second insight suggests that we can reach an even smaller diameter for Au nanorods than for Cu nanorods.

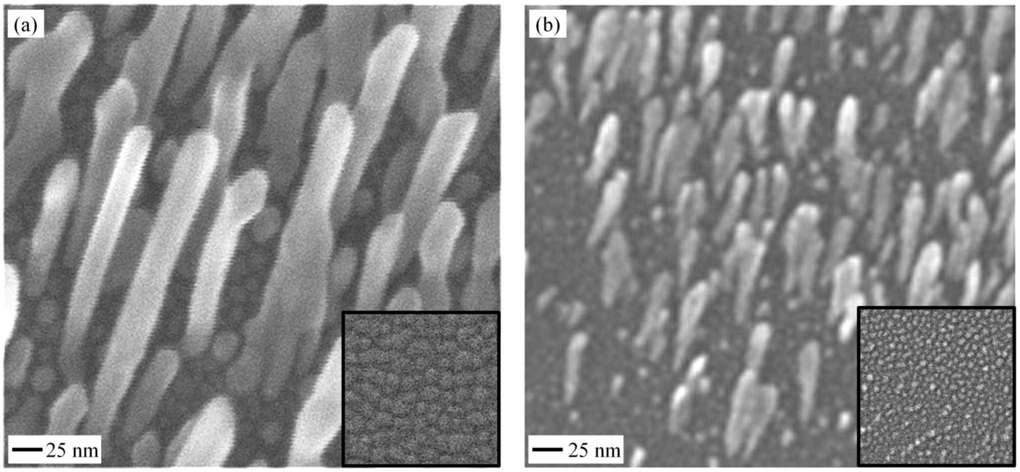

FIG. 3. Scanning electron microscopy images of well-separated (a) Cu and (b) Au nanorods at an early stage; the insets with the same scale show the morphologies of substrates.

Using the first insight from the theory, we design the growth of Cu nanorods as the following, with additional details available in Ref. [17]. We use a large incidence angle of 88°, a substrate with heterogeneous nucleation sites of SiO_2, and a low substrate temperature of about 250 K; the deposition rate is 0.1 nm/s. The experiments indeed confirm that well-separated Cu nanorods of ~20 nm in diameter grow [Fig. 3(a)], as the first theoretical insight suggests. This represents the smallest well-separated Cu nanorods that have ever been reported using PVD. Using both the first and the second insights from the theory, we grow Au nanorods using a large incidence angle of 88°, a substrate that is highly nonwetting (3M copper conductive tape 1182, 3M Corporation, St. Paul, MN), and a low substrate temperature of about 250 K; the deposition rate is also 0.1 nm/s. The experiments indeed confirm that well-separated Au nanorods of ~10 nm in diameter grow [Fig. 3(b)], as the two theoretical insights suggest. In fact, some of the Au nanorods are as small as 7 nm in diameter. Once again, the Au nanorods of ~10 nm in diameter are the smallest well-separated metallic nanorods that have ever been reported using PVD.

As the well-separated nanorods continue to grow beyond ~800 nm in height, they start to form new architectures. For the case of Cu, bridging occurs but nanorods generally remain separated. In contrast, nearly complete merging of nanorods occurs without the heterogeneous nucleation sites [Fig. 4(a) inset]. For the case of Au, branching has occurred beyond ~800 nm, but the small diameter and the separation of nanorods both persist. In contrast, a dense columnar Au film grows when the substrate is a regular Si {100} substrate with native oxide [Fig. 4(b) inset].

In summary, we have formulated a closed-form theory of the smallest diameter of metallic nanorods using PVD, verified the theory using LKMC simulations, and validated

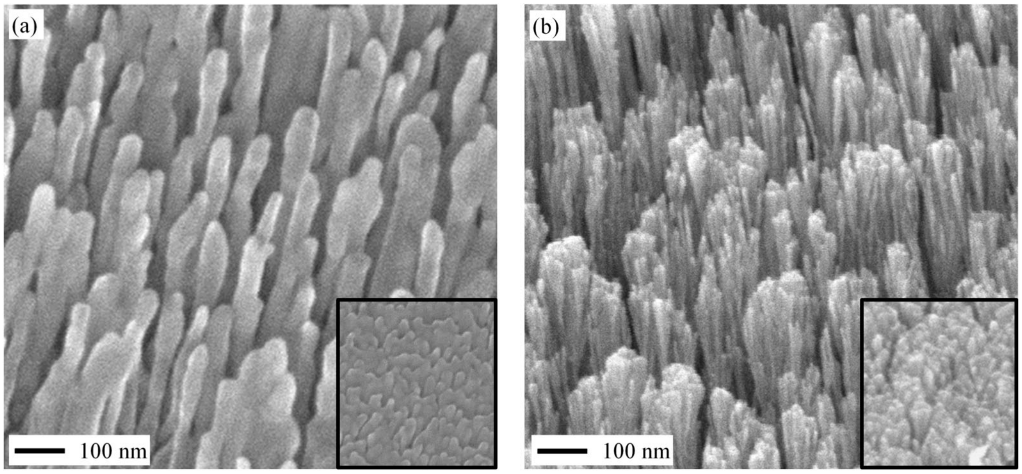

FIG. 4. Scanning electron microscopy images of (a) Cu and (b) Au nanorods at a later stage when nanorods are about 1000 nm long; the insets with the same scale show surface morphologies of nanorods when conventional substrates are used.

it using previous experiments. Further, using the theory-guided PVD experiments, we have realized well-separated Cu nanorods of ~20 nm in diameter and well-separated Au nanorods of ~10 nm in diameter. These Au nanorods are the smallest well-separated metallic nanorods that have ever been reported using PVD.

The authors acknowledge the financial support of the U.S. DOE Office of Basic Energy Science (DE-FG02-09ER46562) and access to user facilities at the Center for Integrated NanoTechnologies at Los Alamos and Sandia National Laboratories. X. N. and S. P. S. contributed equally to this work.

---

*Corresponding author.
hanchen@uconn.edu

[1] K. Robbie, D. J. Broer, and M. J. Brett, Nature (London) **399**, 764 (1999).

[2] T. Karabacak, G.-C. Wang, and T.-M. Lu, J. Appl. Phys. **94**, 7723 (2003).

[3] M. Murdoch, G. I. N. Waterhouse, M. A. Nadeem, J. B. Metson, M. A. Keane, R. F. Howe, J. Llorca, and H. Idriss, Nat. Chem. **3**, 489 (2011).

[4] M. Turner, V. B. Golovko, O. P. H. Vaughan, P. Abdulkin, A. Berenguer-Murcia, M. S. Tikhov, B. F. G. Johnson, and R. M. Lambert, Nature (London) **454**, 981 (2008).

[5] M. Haruta, Nature (London) **437**, 1098 (2005).

[6] P.-I. Wang, S. H. Lee, T. C. Parker, M. D. Frey, T. Karabacak, J.-Q. Lu, and T.-M. Lu, Electrochem. Solid-State Lett. **12**, 138 (2009).

[7] W. K. Burton, N. Cabrera, and F. C. Frank, Phil. Trans. R. Soc. A **243**, 299 (1951).

[8] J. Tersoff, A. W. Denier van der Gon, and R. M. Tromp, Phys. Rev. Lett. **72**, 266 (1994).

[9] J. Krug, P. Politi, and T. Michely, Phys. Rev. B **61**, 14 037 (2000).

[10] H. C. Huang, JOM **64**, 1253 (2012).

[11] R. X. Zhang and H. C. Huang, Appl. Phys. Lett. **98**, 221903 (2011).

[12] R. L. Schwoebel and E. J. Shipsey, J. Appl. Phys. **37**, 3682 (1966).

[13] M. G. Lagally and Z. Y. Zhang, Nature (London) **417**, 907 (2002).

[14] S. K. Xiang and H. C. Huang, Appl. Phys. Lett. **92**, 101923 (2008).

[15] S. H. Lee and H. C. Huang, Nanoscale Res. Lett. **6**, 559 (2011). Following the same method, we have obtained 0.52 eV as the energy barrier of adatom diffusion over multiple-layer surface steps in Au.

[16] L. G. Zhou and H. C. Huang, Phys. Rev. Lett. **101**, 266102 (2008).

[17] See Supplemental Material at http://link.aps.org/supplemental/10.1103/PhysRevLett.110.136102 for detailed derivation, verification, and experimental setup.

[18] S. P. Stagon, H. C. Huang, J. K. Baldwin, and A. Misra, Appl. Phys. Lett. **100**, 061601 (2012).

[19] L. G. Zhou and H. C. Huang, Appl. Phys. Lett. **100**, 141605 (2012).

[20] T. Karabacak, J. S. DeLuca, P. I. Wang, G. A. Ten Eyck, D. Ye, G. C. Wang, and T. M. Lu, J. Appl. Phys. **99**, 064304 (2006).

[21] C. Li, Z. Wang, P.-I. Wang, Y. Peles, N. Koratkar, and G. P. Peterson, Small **4**, 1084 (2008).

[22] G. Ehrlich and F. G. Hudda, J. Chem. Phys. **44**, 1039 (1966).